Proceedings of the Iowa Academy of Science

Volume 64 | Annual Issue Article 37

1957

Soil Stabilization with Large Organic Cations and Polyacids

R. L. Nicholls
Iowa State College

D. T. Davidson
Iowa State College

Soil Stabilization with Large Organic Cations and Polyacids

By R. L. Nicholls and D. T. Davidson

Previous studies at the Iowa Engineering Experiment Station have demonstrated the superior water-proofing ability of large organic cations as soil stabilizing agents (1, 2, 3). A method of combining this water-proofing ability of a large organic cation with the cementing capacity of a polyacid is presently being studied. This report describes the mechanisms of water-proofing and cementing and presents results of the first part of the experimental work.

Water-Proofing Soil with Large Organic Cations

Large organic cations are adsorbed on the negatively charged surfaces of clay minerals and their hydrocarbon groups impede the movement of water through the soil pores. Due to greater van der Waals attraction, the larger cations are generally difficult or impossible to replace by smaller organic cations or by inorganic cations (4). Organic cations are also adsorbed between layers of the expandable lattice minerals of the montmorillonite group (5). They retard changes in the thickness of water films between these layers and thereby reduce swelling and shrinking of the expandable lattice minerals. In general, the larger the organic cation the greater its effectiveness in reducing the water adsorbing capacity of the treated soil (6).

The mechanism by which large organic cations influence the bonding of soil particles by water films may be presented descriptively in the following manner.

A drop of liquid placed between two closely spaced parallel plates assumes a minimum energy configuration which depends upon the force of gravity acting on the liquid and upon interfacial tensions between the gas, liquid and solid phases. If the distance between the two plates is small, the gravity term is negligible and the configuration of the drop may be predicted from interfacial relationships along.

The range of configurations which the drop may assume under the influence of varying contact angles with the two plates is illustrated by use of a soap film analogy in the photographs, Figure 1a to 1d. Two laboratory funnels having their rims coated with a soap solution were brought into superposition and then separated a short distance.*

*A stable soap solution can be made with 60% distilled water, 30% glycerine and 10% triethanolamine oleate. A small amount of titanium dioxide powder gives the film a high index of refraction for better photographic results. This formula developed by Mr. Ray Bonanno of the Theoretical and Applied Mechanics Department, Iowa State College.

The upper funnel was closed to the atmosphere and a variable level water reservoir connected to the lower funnel provided a means of varying the pressure within the soap film. The law of surface tension governing the film tends to minimize its surface area for any given pressure difference across the surface of the film. In Figure 1a the film has been slightly evacuated. In Figure 1b the pressure on both sides of the film is equal and the surface becomes a catenoid, since the minimal curve of revolution is a catenary. Figures 1c and 1d illustrate successive increases of pressure within the film. Figures 1e through 1h represent liquid drops between two parallel plates having the same configurations as the analogous soap films pictured above.

In Figures 1e through 1h the work required to separate the two plates against forces which are caused by the liquid drop may be expressed by the equation:

$$dW/dD = \gamma_{LA}(dS/dD) + (\gamma_{AS} - \gamma_{LS})dA/dD + (P_G - dP_L/dD)(dA/dD) \quad (1)$$

where

dW = work
dD = increase in distance between the two plates
γ_{LA} = liquid-air interfacial tension
dS = increase in liquid-air interfacial area
γ_{AS} = air-solid interfacial tension
γ_{LS} = liquid-solid interfacial tension
dA = decrease in the liquid-solid interfacial area

as represented by the shaded portion of Figure 1j.

The pressure within the liquid differs from that in the gas and the term $(P_G - dP_L/dD)(dA/dD)$ accounts for the work done in moving the plates against this pressure difference (7). The value of $P_G - P_L$ comes from the expression:

$$P_G - P_L = \gamma_{LA}\left(\frac{1}{R_1} + \frac{1}{R_2}\right) \quad (2)$$

where P_G is the gas pressure, P_L is the pressure within the liquid and R_1 and R_2 are the radii of curvature of the surface film in its two principal directions, taking concavity toward the gas phase as positive. If the liquid perfectly wets the two plates, i.e. no contact angle, the liquid-solid interfacial area does not decrease when the two plates are separated. For this special case the second and third terms on the right-hand side of equation (1) drop out.

Assuming comparable values of dS and dA for each of the conditions represented in Figures 1e through 1h, a quantitative comparison may now be made of the work required to separate the two

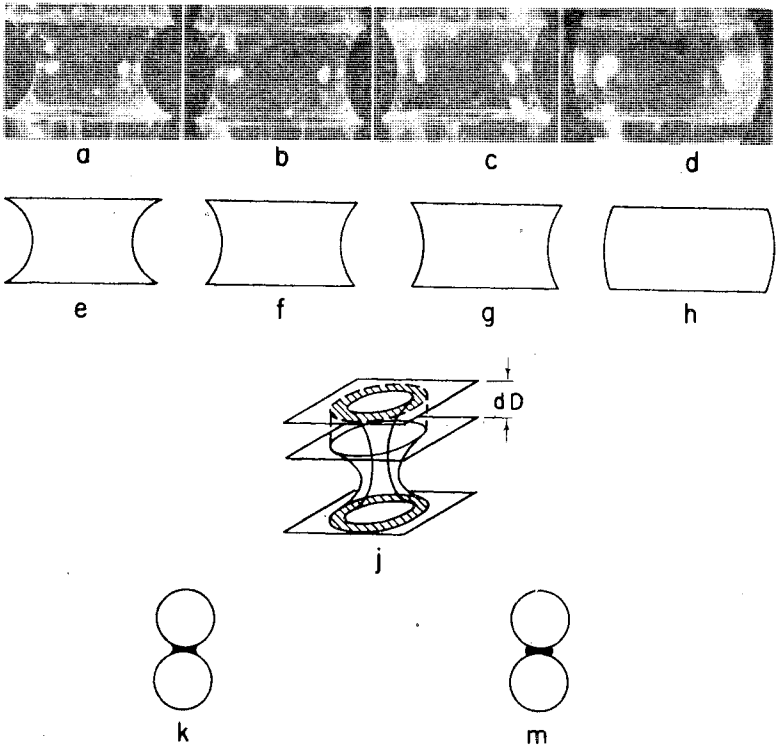

Figure 1. Configurations assumed by liquid drops between two plates and between two spheres for various contact angles. Photographs a to d are soap film analogies for the corresponding sketches e to h.

plates a given distance in each of these four cases. In Figure 1e both of the energy changes due to movement of the triple interface, represented by the last two terms in equation (1), are positive. The term $(\gamma_{SA} - \gamma_{LA})$ is positive because the contact angle is less than 90° and the term $(P_G - dP_L/dD)$ is positive in analogy to the evacuated soap film in Figure 1a. The catenoid of Figure 1f represents a special case in which $R_1 = -R_2$ and the last term of equation (1) drops out. In Figure 1g the term $(P_G - dP_L/dD)$ becomes negative and in Figure 1h both $(P_G - dP_L/dD)$ and $(\gamma_{AS} - \gamma_{LS})$ are negative. These comparisons yield the following relationship:

$$dW/dD_{1e} > dW/dD_{1f} > dW/dD_{1g} > dW/dD_{1h} \qquad (3)$$

showing that any increase in contact angle results in a decrease in the work required to separate the two plates.

If the two parallel plates are replaced by the curved surfaces represented in Figures 1k and 1m the foregoing expressions will still be qualitatively valid. Since the contact angle between water and most mineral surfaces is very small, we may let Figure 1k represent a

water droplet between two idealized mineral particles and Figure 1m represent a water droplet between two similar particles which have been coated with large organic cations.

In order to understand the action of large organic cations as soil stabilizing agents it may first be observed that mechanical failure of a soil mass involves shear planes along which particles roll and slide past one another. If the soil is initially in a compacted state this process requires an increase in the void ratio and a separation of individual particles as the mass becomes dilatent. Figures 1k and 1m and expression (3) show that less work is required to separate the pair of idealized mineral particles coated with large organic cations than to separate the uncoated pair.

Next the work required to separate a group of eight cubically packed spherical mineral particles under different moisture conditions may be considered. In Figure 2a no moisture is present, hence no bonding. In Figure 2b only small annular rings of water are present around the points of contact of the mineral particles. The total liquid-air interfacial area is very small and all water molecules are in close proximity to the two mineral surfaces. Under these conditions, bonding by oriented water dipoles between the charged mineral particles may be large compared with the bond energy due to surface phenomena. As more water is added (Figure 2c) the liquid-air interfacial area is increased and the change in this area, dS, accompanying a given separation dD between the particles also increases. Thus the water bond energy in this range of moisture content is increased by the addition of water. As more water is added, however, the interior void between the eight spheres may become filled (Figure 2d). A comparison of Figures 2e and 2f, which represent top views of figures 2c and 2d respectively, illustrates the decrease in total peripheral length of water film (dotted lines) connecting the two planes of four spheres due to filling the interior void with water. The ratio dS/dD is therefore lower for Figure 2d than for Figure 2c and the water bond energy has been reduced. Figure 2g represents total immersion of the eight spheres in water. For this case no liquid-air interfaces exist and any water bonding must again be due entirely to oriented water dipoles in close proximity to any two charged mineral surfaces.

Figure 2h illustrates the state of water bonding when random areas of the eight mineral spheres are coated with large organic cations. It becomes apparent that the maximum bond energy represented by Figure 2c can never be realized when part of the mineral surfaces are coated with large organic cations because the water-organic cation interfaces represent areas for which reduced energy is required to separate the particles. However, the presence of the

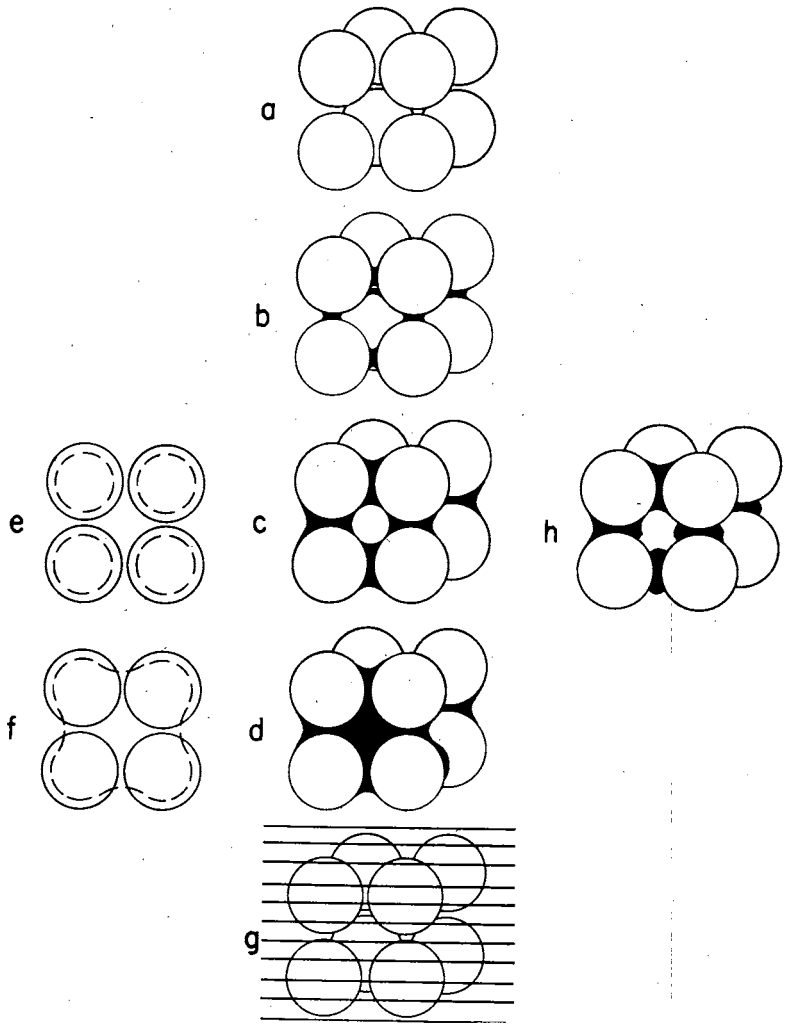

Figure 2. Effects of moisture content and of partial coating with a surface active agent on the bonding of eight cubically-packed spherical particles by water.

large organic cations may prevent a transformation to the condition of Figure 2d by inhibiting the entrance of additional moisture into the central void.

These interpretations appear to be substantiated by the results of mechanical strength tests performed after air-drying and after immersion of soils stabilized with large organic cations. Air-dry strengths are decreased by the addition of large organic cations whereas immersed strengths are greatly increased. At higher percentages of treatment, however, the immersed strengths also de-

crease (Figure 10, p. ... and reference 3). These results indicate that a percentage of treatment exists above which the beneficial effect of restricting the entrance of additional water during immersion of the soil is exceeded by the detrimental effect of reduced bond energy resulting from the increase in water-organic interfaces.

This presence of an optimum quantity of large organic cations also attests to the relatively high bond energy of water films compared to any bonding action which can be attributed to van der Waals attraction between large organic cations near the points of contact of the mineral particles.

In addition to coating the exterior surfaces of mineral particles and restricting moisture movements through the soil pores, large organic cations are absorbed between layers of the expandable montmorillonite minerals. Their stabilizing action here depends upon a somewhat different principle. By minimizing changes in the thickness of water films between these layers they reduce fractures caused by differential swelling and shrinking throughout the soil mass.

Cementing Soil Particles with High Polymers

High polymers, unlike large organic cations, increase the air-dry strength of soils (8). Bond action apparently depends upon both air-water interfaces and upon the cementing action of the polymer.

In recent years a fairly rigorous theoretical analysis has been made by systems in which the elastic properties of high polymers are improved by the inclusion of small amounts (usually below 25%) of mineral fillers (9-12). Mathematical expressions to characterize these systems have been developed from the classical derivation of Einstein (13, 14) and a subsequent modification by Guth and Gold (15) which are based on the energy required for the displacement of a fluid around rigid disperse particles.

Apparently no similar analysis has been made of systems in which the mineral phase predominates, i.e., where intergranular contacts exist and where the voids are not completely filled with high polymer. This is the condition in soils stabilized with high polymers. For cases where the mineral phase predominates, an analogous solution might be obtained by expressing the shear behavior of the rigid particles as a function of alterations due to inclusion of the polymer, rather than characterizing the fluid phase in terms of perturbations due to the inclusion of rigid particles.

The resistance to shear of a granular material may be expressed by the equation:

$$S = N \tan \theta \qquad (4)$$

where S is the shear strength, N is the intergranular pressure normal

to the shear plane and θ is the angle of internal friction of the granular material. If there are interparticle forces operating independently of N, the equation becomes

$$S = C + N \tan \theta \qquad (5)$$

the Coulomb equation in which C is the cohesion. Although the physical significance of cohesion is quite complex, a portion of this term can be attributed to the resistance to dilation during shear which is offered by the large air-water interfacial areas in fine grain soils. This mechanism was discussed in the previous section.

A typical stress-strain curve from a direct shear test on dense sand is illustrated in Figure 3. As indicated, the maximum shear stress of a dense sand often occurs about midway between zero strain and the strain at which maximum dilatency is developed. This behavior is typical of dense fine grain soils as well.

An organic polymer in soil may decrease the total air-water interfacial area, and therefore decrease that portion of cohesion attributed to water bonding. On the other hand, the polymer contributes cementing action of its own which is apparently a function of the density of polymer chains crossing the shear plane, their orientation, Young's modulus of the chains in tension, and the lengths of chains between points on each side of the shear plane which are relatively fixed, such as between branch points in a polymer network.

Methods of employing a given amount of polymer in the soil to achieve maximum shear strength may be visualized in various ways. Two theoretical advantages accrue from having the polymer chains connect directly between soil particles, as in Figure 4b instead of passing around the particles, as in Figure 4a. In Figure 4b, the soil particles themselves constitute portions of the polymer network. According to this scheme a polymer network may be visualized in which the branch points have been magnified many times and replaced by soil particles. The smaller the void ratio of the soil, the greater will be the effective portion of soil particles in the polymer networks. By this method a greater number of chains (composite chains comprised of both polymer and soil particles) are made to cross any shear plane with a given amount of polymer.

A second theoretical advantage of polymer bonding directly to neighboring soil particles is the effect of such a system in decreasing the average length of polymer chains between fix points. In Figure 5 two polymer chains crossing the shear plane b-b at an angle θ have different lengths between fix points on opposite sides of the shear plane. For a given shear displacement S, $d'/d > D'/D$. If both chains have the same Young's modulus the shorter chain will therefore offer the greater resistance to shear. Ideally, a relationship

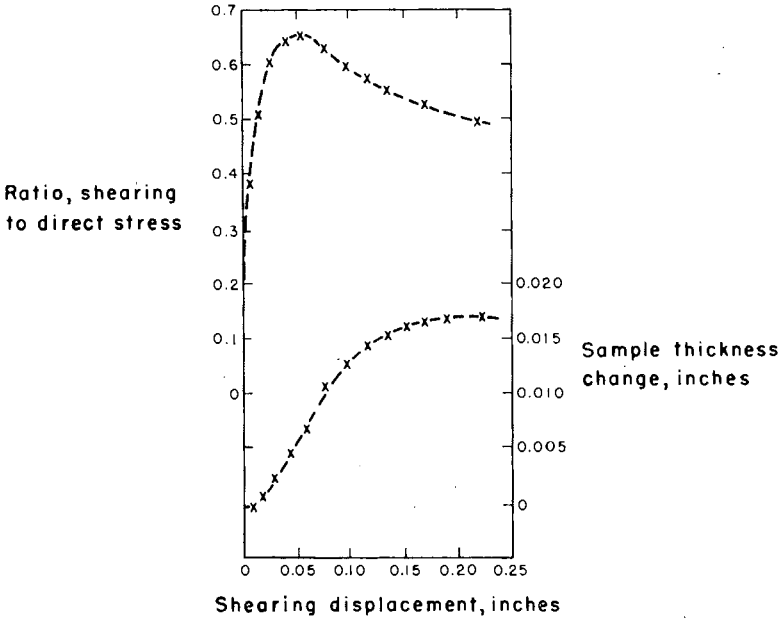

Figure 3. Typical plot of a direct shear test for dense sand. (Taken from Fundamentals of Soil Mechanics, by Donald W. Taylor.)

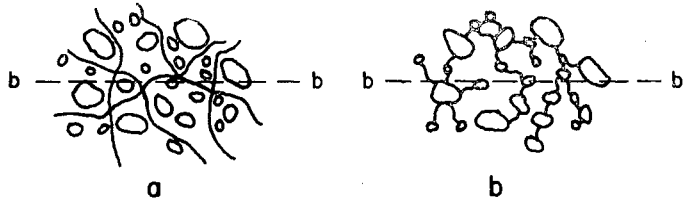

Figure 4. Comparison of the effectiveness of a non-bonded soil-polymer system (a) with a bonded soil-polymer system (b) in resisting shear across the surface b-b.

may exist in which the average length of polymer segment between fix points is such that maximum retractive stress of the polymer will be attained at the same shear strain at which the maximum internal friction stress indicated in Figure 3 is developed.

The realization of both of these advantages depends upon the formation of bonds between the soil particles and polymer which are at least as strong as those within the polymer. Bonds between soil particles and polymer might be van der Waals, ionic or covalent in nature. Interesting examples of ionic and covalent bonding between polymer and dispersed mineral particles are found in the field of rubber technology. Havenhill and coworkers (16) discovered that when highly positive fillers are milled into rubber, which is itself very negative, the strong electrostatic bonds formed gave rise to

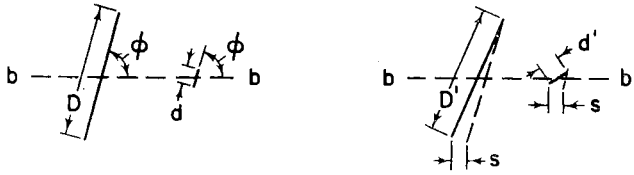

Figure 5. Resistance offered by a single polymer chain to shear across the surface b-b as a function of length of the polymer chain between fix points.

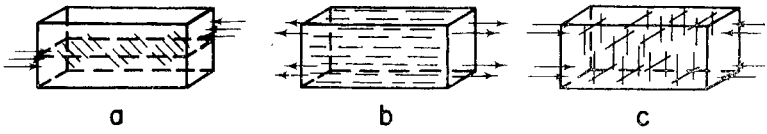

Figure 6. Optimum orientations of polymer chains in a soil subjected to different types of stress: (a) shear, (b) tension, and (c) compression.

additional increases in modulus of elasticity and tensile strength. By this method, the tensile strength of pure gun GR-S stocks was increased more than fivefold. Sterns and Johnson (11) found that when rubber containing carbon black is vulcanized using sulfur and accelerators extensive chemical bonding of polymer to the mineral surfaces occur. The bonds so formed constitute additional points of constraint and increase the modulus of elasticity beyond that of a system having no bonding between polymer network and mineral particles.

In connection with this relationship, in which maximum retractive tensile stress of the polymer and maximum frictional shear resistance between mineral particles are developed simultaneously, another possibility may also be observed. If an initial tensile stress can be induced in the polymer, the initial shear displacement will require greater external force and the system will assume a character analogous, on an infitismal scale, to that of prestressed reinforced concrete.

Finally, greater strength might be obtained with the same amount of polymer if the polymer chains could be oriented in such a manner as to most effectively resist a given type of applied stress. In the field of rubber technology the phenomena of chain orientation due to imposed strains has received considerable attention. For example, Flory and coworkers (17) have developed an equation for the proportion of randomly distributed chains which are lengthened as a function of deformation in a stretched rubber and have studied the relationships between degree of cross-linking, orientation due to strain, and maximum tensile strength of rubbers.

For a soil-polymer system subjected to direct shear, preferential orientation of the polymer chains might be represented by the slanted lines in Figure 6a. The orientation shown for simple tension (Figure

6b) and simple compression (Figure 6c) are apparent from a consideration of elementary mechanics.

In summary, the theoretically ideal conditions for maximum utilization of a polymer in soil appear to be:

1. Direct bonding between neighboring soil particles.
2. Pretensioning of polymer chains.
3. Orientation of polymer depending upon the external stresses to be resisted.

Methods of attaining the first two of these three conditions are presently being studied and will be described in the experimental section. General mathematical expressions for the above relationships are outlined in the following paragraphs.

Imagine that each of three soil samples, row 1 of Figure 7, is subjected to a shear displacement dD. Since shear failure in granular materials takes place within a zone instead of on a unique plane, the shear planes indicated in the samples may be considered as planes within a shear zone. Sample 1a will be stabilized with polymer having an initial average distance between fix points. The fix points may be either branch points in a polymer network or bonds connecting the polymer to soil particles. Sample 1b will be identical to 1a except that the initial average distance between fix points will be less than L. Sample 1c will be identical to 1b except that an initial tension shall be placed in the polymer chains prior to the shear displacement dD. A random initial orientation of polymer segments in each of the three samples will be assumed.

In row 2, Figure 7, each polymer agent crossing the shear planes in the three samples has been projected into the plane of the paper and placed on the abscissa scale according to the angle which the projected segment makes with the shear plane. When the samples are subjected to a shear displacement dD, those segments between 90° and 180°, row 2, will not be lengthened and therefore will undergo no tensile stress. The tensile stress developed in segments lying between 0° and 90° can be expresed by the equation:

$$S' = \frac{L' - L}{L} Y \qquad (6)$$

where S′ is the tensile stress per polymer segment, L and L′ are the initial and final lengths of the segment between fix points on opposite sides of the shear plane, and Y is the Young's modulus of the segment in tension. Flory (18, Ch. XI) presents a comprehensive analysis of the factors governing the Young's modulus of polymer systems.

In row 3 the tension vectors of the polymer segments parallel to the direction of shear are shown as a function of ϕ, the angle between

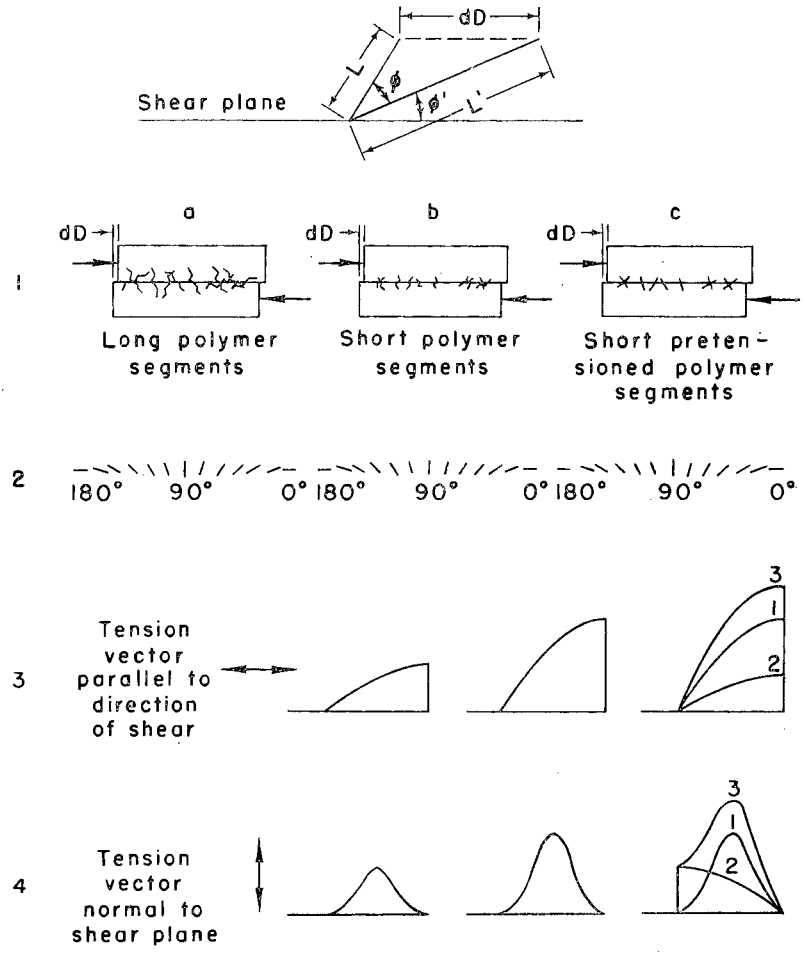

Figure 7. Tension vectors of randomly oriented polymer segments crossing a shear plane as functions of segment length between fix points and pretensioning.

the projected segment and the shear plane. These curves are obtained from the expression:

$$[3] = S' \cos \phi' = \left(\frac{L' - L}{L} Y\right) \cos \phi' \qquad (7)$$

where [3] designates the tension vector parallel to the shear plane and ϕ' is the adjusted angle ϕ after the sample has been subjected to shear strain. From the sketch at the top of Figure 7, and by the law of sines,

$$L' = \frac{L \sin (180 - \phi)}{\sin \phi'}$$

$$\sin \phi' = \frac{L \tan \phi}{dD + L \cot \phi}$$

$$L' = \frac{L \sin (180 - \phi)}{\frac{L \tan \phi}{dD + L \cot \phi}} = \cos \phi \, (dD + L \cot \phi)$$

and

$$\cos \phi' = \sqrt{1 - \sin^2 \phi'} = \sqrt{1 - \left(\frac{L \tan \phi}{dD + L \cot \phi}\right)^2}$$

Introducing these values into equation (7),

$$[3] = Y \left[\frac{\cos \phi \, (dD + L \cot \phi) - L}{L}\right] \sqrt{1 - \left(\frac{L \tan \phi}{dD + L \cot \phi}\right)^2} \tag{8}$$

As this equation indicates, the ordinate values of graph 3b are greater than those in 3a due to the shorter polymer segment length in sample (b). Curve 2 in graph 3c represents the stress parallel to the direction of shear due to pretensioning the polymer segments, expressed by the equation:

$$[3c2] = S \cos \phi \tag{9}$$

where S is the pretension stress per polymer segment. Curve 3 in graph 3c represents the total tension parallel to the direction of shear due to pretensioning plus shear displacement.

Row 4 represents the tension vectors in the polymer segments normal to the shear plane, expression by the equation:

$$[4] = S' \sin \phi'$$

$$= Y \left[\frac{\cos \phi \, (dD + L \cot \phi) - L}{L}\right] \left[\frac{L \tan \phi}{dD + L \cot \phi}\right] \tag{10}$$

The contribution of the prestress tension in this case, represented by curve 2 in graph 4c, is

$$[4c2] = S \sin \phi \tag{11}$$

To find the components of total tension normal and parallel to the direction of shear the curves in rows 3 and 4 respectively may be integrated between the limits of 0° and 90°. Analogous to the basic Coulomb equation we then obtain:

$$S = C - c + N \tan\theta + \tan\theta \int_0^{90°} [4] + \int_0^{90°} [3] \tag{12}$$

where S is the applied external shear stress at any value of shear strain, c is the reduction in water-air interfacial bond energy due to the presence of the polymer, and the other quantities are as desig-

nated previously. Maximum shear strength is developed at the strain at which a combination of the five terms in equation (12) obtains a maximum.

Properties of Polyelectrolytes

As the experimental work deals primarily with the dilation and contraction of polymeric electrolytes and with the formation of metal chelates a brief outline of these two fields will be presented in the following paragraphs.

Dilation and Contraction of Polymeric Electrolytes

Polymeric electrolytes, commonly called polyelectrolytes, are a class of high polymer molecules having ionizable groups as part of their repeating unit. Electrochemically, the polyelectrolytes include polyacids, polybases, and polyampholytes. The polyampholytes contain both acidic groups and basic groups.

The mechanism of swelling of ionic polymers, presented by Flory (18, pp. 584-598, 629-637) and others (19-23), may be explained on the basis of either of two mutually related phenomena: electrostatic repulsion and osmotic pressure. Expressions for the swelling of linear ionic polymers based upon the electrostatic repulsion concept have been derived by Katchalsky and coworkers (20). For the sake of brevity the osmotic pressure concept developed by Flory will be presented here.

When a polyelectrolyte is ionized, as for example when polyacrylic acid in dilute aqueous solution is neutralized with sodium hydroxide (Figure 8), the concentration of the mobile sodium ions will always be greater in the gel than outside because of the attracting power of the fixed negatively charged carboxyl groups. Consequently the osmotic pressure of the solution inside will exceed that of the external solution and the expansion force may be equated to these differences in osmotic pressures of the two solutions. The osmotic pressure (18, p. 587) arising from the difference in mobile ion concentrations between the gel and the external solution will be:

$$\pi_i = RT\,[C_+ + C_- - (C_+^* + C_-^*)] \qquad (13)$$

where

π_i = the difference in osmotic pressure caused by the difference in mobile ion concentrations.

R = gas constant.

T = absolute temperature.

$C_+ + C_-$ = total mobile ion concentration inside the gel at equilibrium.

$C_+^* + C_-^*$ = total mobile ion concentration outside the gel.

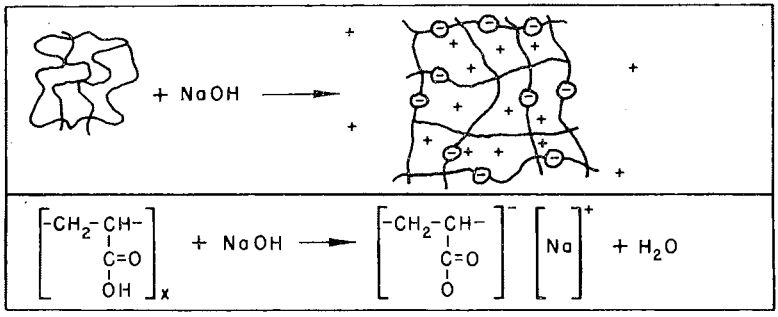

Figure 8. Neutralization of a polyacrylic acid gel in dilute aqueous solution with sodium hydroxide.

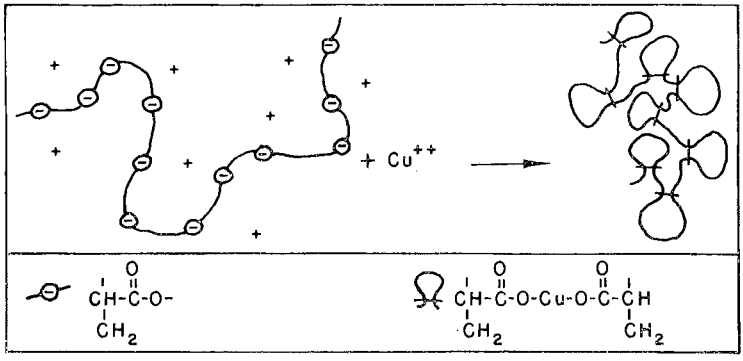

Figure 9. Contracting and water-proofing a polyacid by chelation with a transition metal.

If a polyacid gel is highly ionized the C_+ term (in the case of our example, the sodium ions within the gel) will increase in an effort to maintain electro-neutrality within the gel, causing a greater expansive force π_i. When a small concentration of a salt such as sodium chloride is added to the solution the concentration of the internal mobile ions $C_+^* + C_-^*$ increases relative to the concentration of the external mobile ions $C_+ + C_-$ and the expansive force π_i is greatly reduced. The gel, though still ionized, returns to the randomly kinked configuration indicated at the left of Figure 8.

Katchalsky and Zwink (*22*) found that transferring polyelectrolyte fibers from one solution to another of higher chemical potential required a larger force to maintain the length of the fibers constant. Thus when polymethacrylic acid fibers held at a constant length were transferred from a solution of sodium hydroxide to one of barium hydroxide, tensile stresses were induced in the fibers. Exploiting this relationship to provide the pretension stress in equations 9, 11 and 12 is one of the experimental objectives of this study.

Chelation of Polyacids

Whereas the ionic character of polyacids permits a manipulation of dilation and contraction, it is also responsible for an undesirable feature, water affinity. An ideal solution to this problem would be to find a way to bond the polymer to adjacent mineral particles, and then alter it in a way to accomplish both tensioning and water-proofing of the polymer chains. Fortunately the tensioning and water-proofing appear possible by the reaction between polyacids and transition metals such as iron, copper, zinc and nickel. These metals react to produce essentially covalent bonds between neighboring ionized acid groups as illustrated in Figure 9.

Many cations other than the transition metals react with strong electron donors such as nitrogen, sulfur and oxygen to form similar ring structures in which the metal bonds are essentially ionic. The term chelate is applied to these ring structures whether the metal bonds are esentially ionic or covalent. Chelates in which the metal bonds are essentially covalent are termed inner-complex salts (24).

Martell and Calvin (24, p. 183) point out that the factors which govern the relative tendencies for various metals to combine with a given electron donor may be divided into two classes: (1) the ionic forces which are related to both charge and radius of the metal ion, and (2) the relative tendencies of various metals to form homopolar bonds with electron donors. Regarding class (1), studies of ion exchange equilibria in polyelectrolytes (25) have shown general agreement with the results of the classical Hoffmeister-series investigations. More highly charged ions are generally adsorbed in preference to those of less charge and among ions of the same charge, those having smaller hydrated radii are usually adsorbed in preference to those of larger hydrated radii. Regarding class (2), Mellor and Maley (26) pointed out that as a first approximation the stability of metal chelates seems to decrease with increasing basicity of the metal, weakly basic copper forming the strongest, and the most strongly basic metal, magnesium, forming the weakest chelates. Thus the metals which can form the strongest homopolar bonds generally form the most stable chelates.

Experimental

The objectives of the experimental work were to evaluate the use of polyacids with large organic cations for soil stabilization and to study the possibility of chelating the polyacids at a reaction rate low enough to permit ionic bonding of the polyacids to the large organic cations coating the mineral surfaces before final water-proofing and tensioning of the polyacid chains.

For purposes of study one soil, a silty loam C-horizon loess, and one large organic cationic material, Arquad 2HT, were used. Arquad

2HT, a quaternary ammonium chloride, was chosen on the basis of previous tests indicating its ability to restrict moisture movements in the soil (3). The properties of the loess, of Arquad 2HT and of nine polyacids and polyacid salts used as additives are tabulated in the Appendix.

Soil specimens were prepared and tested by the following procedure:

1. Add Arquad 2HT in aqueous suspension to 700 grams of the soil and mix in a Hobart model C-100 mixer.

2. Add the desired polyacid in aqueous solution or aqueous emulsion to the soil and continue mixing; the total water added in steps 1 and 2 being enough to bring the soil to optimum moisture content for standard Proctor density.

3. Mold the soil in four 2-inch diameter by 2-inch high specimens compacted to near standard Proctor density.

4. Air cure the specimens for seven days and test two of the specimens in inconfined compression.

5. Immerse the remaining two specimens in water for 24 hours before testing them in unconfined compression.

Figure 10 shows the compressive strength of the soil as a function of Arquad 2HT as the only additive. Arquad 2HT hydroxide, represented by the solid line in Figure 10, was prepared by mixing equivalent amounts of potassium hydroxide and the quaternary ammonium chloride in isoproponol and filtering off the precipitated potassium chloride. For later investigations Arquad 2HT hydroxide was obtained from Armour and Company, Chicago, Illinois. As indicated in Figure 10 the chloride and hydroxide forms of Arquad 2HT yield approximately equal strengths, a slight decrease in the immersed strengths occurring above 0.2% treatment in each case. The percentages of treatment indicated in Figure 10 and subsequent graphs are based on the solid weights of chemicals added in solution.

In contrast to the Arquad 2HT treated soil, specimens treated with 0.6% of the various polyacids and polyacid salts all slaked in water. The air-dry strengths of most of these specimens were about one and one-half times the air-dry strength of the untreated soil.

When Arquad 2HT chloride was mixed in dilute aqueous solution with the various polyacids disperse floccules were formed. When Arquad 2HT hydroxide was mixed with the polyacids the floccules formed were much denser and precipitated more quickly than those formed with Arquad 2HT chloride, showing the added effect of ionization of the polyacid by hydroxyl ions in bringing the polyacid and organic cations together. Van der Waals attraction between the

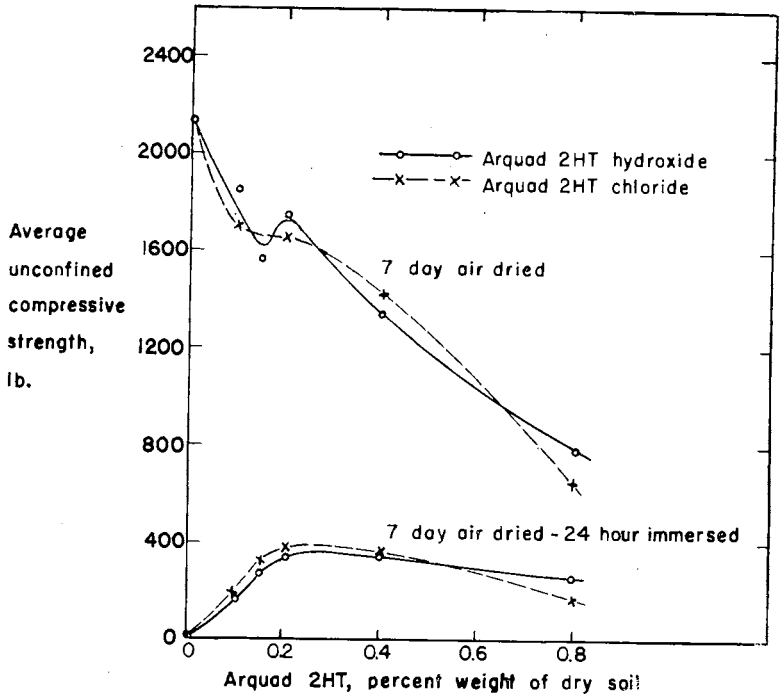

Figure 10. Effect of amont of Arquad 2HT on unconfined compressive strength of the soil. Test specimens were 2 inches in diameter and 2 inches high.

polyacid and the long chain cations is apparently responsible for the stability of the floccules in each case. These results are in substantial agreement with the behavior of similar systems studied by Iler (27), Kressman and Kitchener (28) and Terayama (29). Iler found that mixtures of long chain quaternary ammonium ions with polymetaphosphoric acid were readily precipitated from aqueous solutions as gummy solids. Kressman and Kitchener observed that the affinity of certain large organic cations, including quaternary ammonium salts, for a polyanionic resin increases with increasing size of the cation, also suggesting the importance of van der Waals attraction.

The compressive strengths of the soil treated with 0.2% Arquad 2HT plus 0.6% of the various polyacids and polyacid salts are shown in Figure 11. All strengths in Figure 11 and the following graphs are immersed strengths. The three polyacids giving best results, Acrysols A-1, A-3 and A-5, are members of a homologous series of polyacrylic acids. Acrysol A-1, having the lowest molecular weight, gave the greatest strength, whereas Acrysol A-5, having the highest molecular weight, gave the lowest strength of the three.

One factor which may contribute to this inverse relationship between molecular weight of the polyacid and strength of the stabilized

soil is the effect that polyacid chain length would have on the probability of a polyacid molecule coming to rest between two organic cations. Assuming the mineral surface area for one cation exchange position is 80 A^2 (30, p. 134) and that the organic cations lying flat on the mineral surfaces (4) each occupy 120 A^2, the organic cations cover only 5.8% of the area represented by exchangeable cation positions alone. Although no distinction was made between interlayer cation exchange positions and cation exchange positions on the exterior surfaces in arriving at this value, it may, nevertheless, give some idea of the area covered by the organic cations. It is significant in illustrating that, for a random distribution, the probability of two organic cations on neighboring mineral particles being in close proximity is quite small. In the process of mixing, the number of cation-polyacid-cation bonds formed would seem to be a function of the number of polyacid molecules, the portion of mineral surface area covered by the organic cations, and the nature and time of mixing. For a given weight of polyacid added to the soil the number of molecules coming to rest between adjacent organic

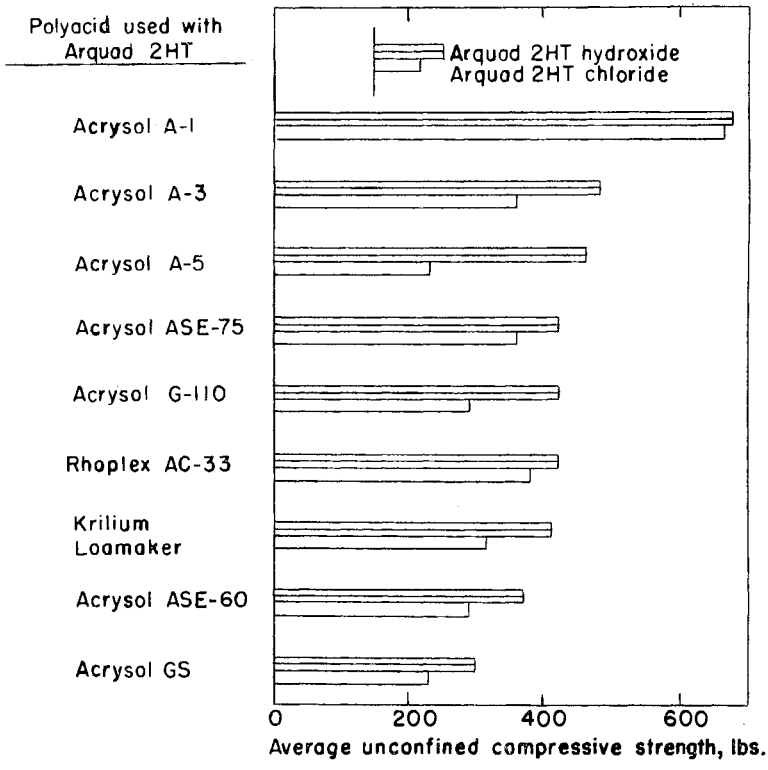

Figure 11. Unconfined compressive strengths of the soil treated with 0.6% of various polyacids and polyacid salts and 0.2% of either Arquad 2HT hydroxide or Arquad 2HT chloride. Strengths of 2-inch diameter by 2-inch high specimens measured after 7-day air drying plus 24-hour immersion.

cations will be statistically greater for the lower molecular weight fraction of polyacid. Theoretically, it appears that for a given weight of polyacid the strength of the treated soil should increase with decreasing molecular weight to a point where the average polymer chain becomes shorter than the length required to bridge the mean gap between two neighboring organic cations.

The Arquad 2HT hydroxide was found to produce greater strength with each of the polyacids than did Arquad 2HT chloride (Figure 11). In agreement with the results of flocculations in aqueous solution, the hydroxyl ions apparently ionize the polyacid groups and thereby increase ionic bonding between the polyacids and organic cations in the soil.

Since Arquad 2HT is commercially available as a chloride salt the possibility of using the chloride form and adding inorganic bases such as sodium hydroxide and potassium hydroxide was investigated as an alternative to using Arquad 2HT hydroxide. Figure 12 shows the strength of the soil treated with 0.2% Arquad 2HT chloride plus 0.6% Acrysol A-1 as a function of the amounts of sodium and potassium hydroxides added with the Acrysol A-1. In comparing the sodium hydroxide and potassium hydroxide curves it may be recalled that the sodium ions, being highly hydrated at high moisture contents, act as a strong dispersing agent in most soils whereas potassium ions do not. In the case of sodium hydroxide the increased bonding of polyacid to cations caused by ionization of the polyacid by hydroxyl ions is apparently offset by the dispersing action of sodium ions. The lower strength of the soil treated with Arquad 2HT and Acrysol GS, the sodium salt of Acrylic acid (Figure 11)

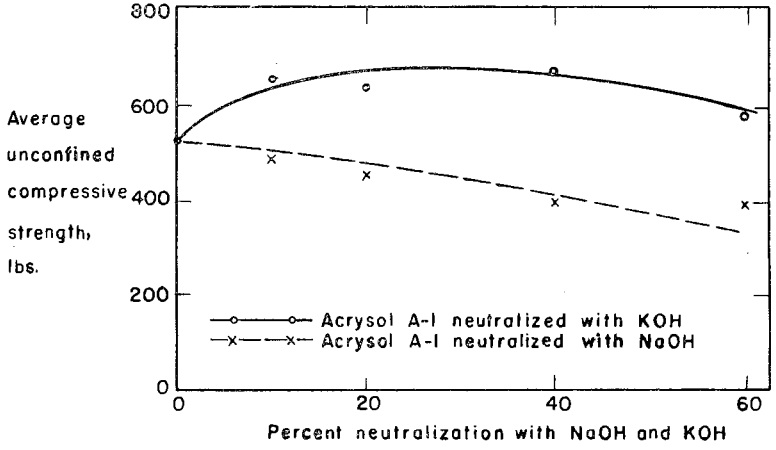

Figure 12. Unconfined compressive strengths of the soil treated with 0.2% Arquad 2HT chloride and 0.6% Acrysol A-1 as a function of percent neutralization of Acrysol A-1 with NaOH and KOH.

might also be partly due to this phenomena. Potassium on the other hand is not a strong dispersing agent and higher strengths occur throughout the entire potassium hydroxide range, indicated by the solid line in Figure 12.

For comparison with the results of Figure 12 similar curves were obtained by replacing the Arquad 2HT chloride with Arquad 2HT hydroxide (Figure 13). As indicated, the Arquad 2HT hydroxide gave strength values slightly greater than those for Arquad 2HT chloride.

To test the theory that the strength of the stabilized soil is a function of the number of cation-polyacid-cation bonds formed between neighboring mineral particles compressive strengths were measured for wide ranges of both Arquad 2HT hydroxide content and Acrysol

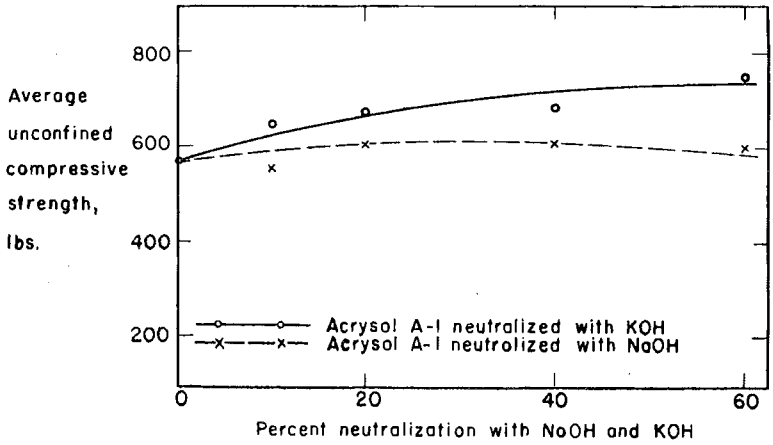

Figure 13. Unconfined compressive strengths of the soil treated with 0.2% Arquad 2HT hydroxide and 0.6% Acrysol A-1 as a function of percent neutralization of Acrysol A-1 with NaOH and KOH.

A-1 content (Figure 14). It is interesting to compare the curves for immersed strength in Figure 10 with the strength contour curves in Figure 14. When Arquad 2HT is used alone (Figure 10) an optimum amount or Arquad 2HT is reached for maximum immersed strength whereas when Arquad 2HT is used with polyacrylic acid (Figure 14) an increase in Arquad 2HT content from any point on the graph yields an increase in immersed strength. Apparently when Arquad 2HT and polyacrylic acid are used together the increase in strength contributed by cation-polyacid-cation bonds, as more Arquard 2HT is added, outweighs the decrease in bonding by moisture films. The strength contours over most of the area in Figure 14 are roughly parallel to the Acrysol A-1 axis. Apparently the concentration of organic cations is a much more critical factor in establishing cation-polyacid-cation bonds throughout the range of additives

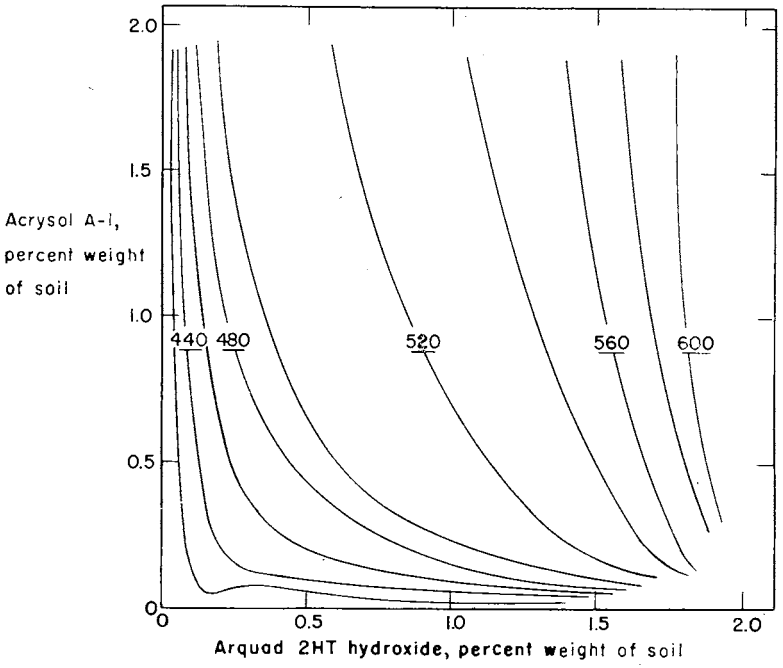

Figure 14. Contours showing the relationship of unconfined compressive strength of the soil to Arquad 2HT hydroxide and Acrysol A-1 contents. Contours indicate 20-lb. increments of strength for 2-inch high by 2-inch diameter soaked specimens.

investigated than is the concentration of polyacrylic acid molecules.

Having obtained a sketchy understanding of the behavior of large organic cations and polyacids in the soil the next step was to study the effect of chelation on the contraction and water-proofing of polyacid molecules. Since Acrysol A-1 gave the highest strengths this polyacid was chosen for chelation studies.

First, the degree of expansion of Acrysol A-1 molecules as a function of neutralization with sodium hydroxide, in accordance with the principal outlined on page 16, was determined by viscosity measurements and by the use of the equation:

$$\alpha^3 = \frac{[\eta]}{[\eta]_0} \qquad (14)$$

where α^3 is the volumetric expansion factor of the polymer molecules, $[\eta]$ is the intrinsic viscosity of the polymer in the presence of sodium hydroxide or other reagent causing a dimensional change and $[\eta]_0$ is the intrinsic viscosity of the unperturbed polymer (31). Viscosities were measured with an Ostwald viscometer at 30° C. (flow time of water = 2 min. 56 sec.). Figure 15 shows the linear expansion factor α as a function of the percent neutralization with

sodium hydroxide and Figure 16 shows the expansion factor for 100% neutralized Acrysol A-1 extrapolated to zero concentration.

In order to determine which inorganic cations produce greatest contractions of the ionized polymer, and hence greatest tensile stress in the polymer chains after bonding to organic cations in the soil, viscosity measurements were made of neutralized Acrysol A-1 in the presence of various salts. The results of these tests are presented in Figure 17. The fact that ferric chloride, added even in very small amounts, precipitates Acrysol A-1 at the concentration used is strong evidence for formation of an inner complex salt. The only ionic groups in Acrysol A-1, the $-COO^-$ groups, have apparently been rendered inactive by covalent bonding with iron, causing water-insolubility.

Metal chelates are formed by the displacement of acidic protons of the chelating agent by metal ions. Thus, addition of a metal salt to the polyacid causes a drop in pH, and the greater the tendency for the metal to combine with the polyacid, the greater the drop in pH. This constitutes a simple method of testing for chelation and it can be used to determine the tendency of different metals to combine with the polyacid.

The results of pH measurements obtained by titrating Acrysol A-1 with these same salts, Figure 18, are in close agreement with the results of the viscosity measurements, Figure 17. It is obvious from Figure 18 that the ferric chelate is very strong whereas the tendency for the alkaline earth metals, magnesium, calcium and barium, to form chelates is quite weak. All metal ions assume approximately

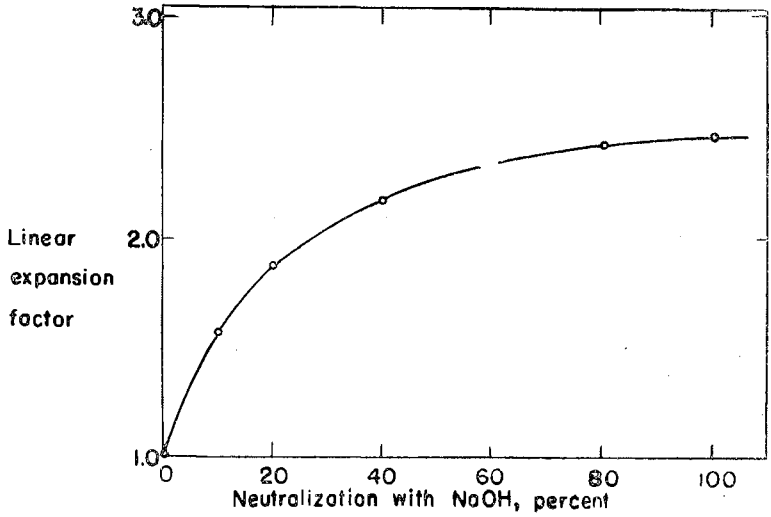

Figure 15. Linear expansion factor of Acrysol A-1 in 0.5% aqueous solution as a function of percent neutralization with sodium hydroxide.

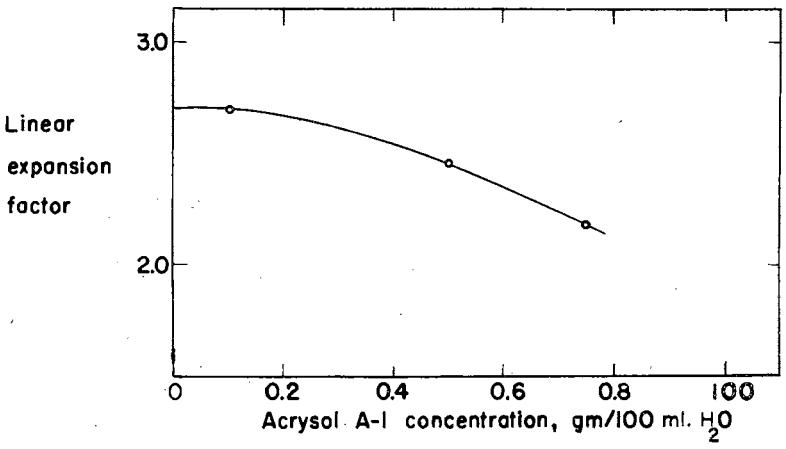

Figure 16. Linear expansion factor of Acrysol A-1 100% neutralized with NaOH as a function of concentration.

the same relative positions in Figures 17 and 18 with the exception of the ferrous ion. Since the data in Figure 17 were obtained for 80% neutralization of the polyacid whereas Figure 18 represents no neutralization, this displacement of the ferrous curve may indicate a greater pH dependency for ferrous chelate formation than for chelation with the other ions investigated.

A comparison of the distances H_1 and H_2 in Figure 19 indicates that a given amount of copper causes greater contraction of the poly-

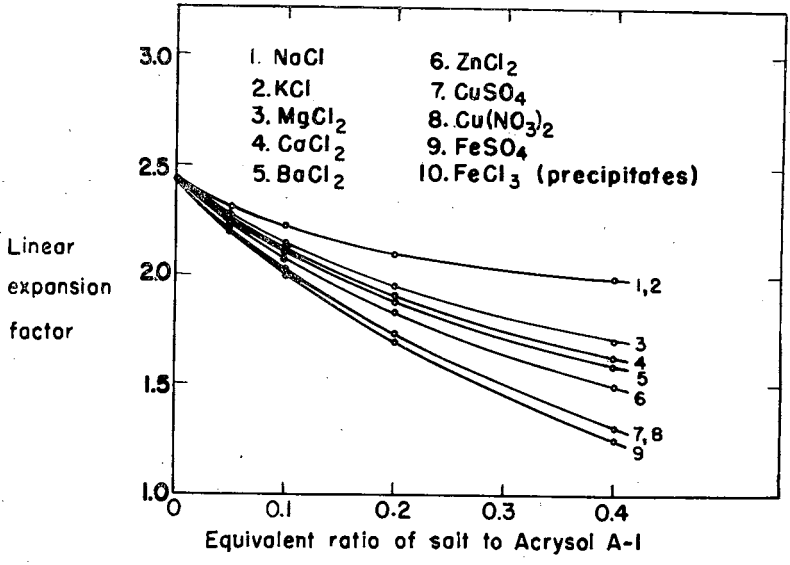

Figure 17. Linear expansion factor of Acrysol A-1 in 0.5% aqueous solution 80% neutralized with sodium hydroxide in the presence of various salts.

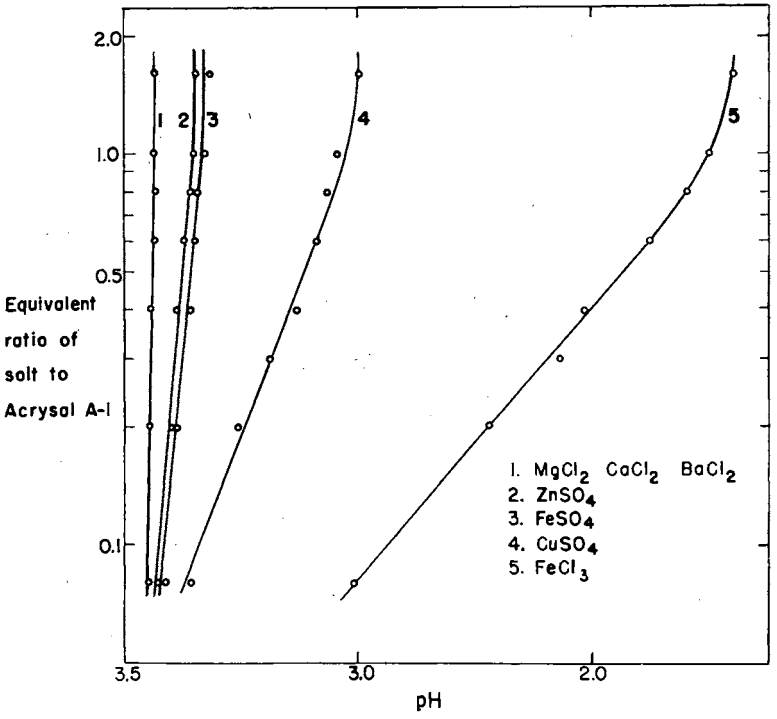

Figure 18. pH titration curves for 0.0116 N. Acrysol A-1 solution with various salts.

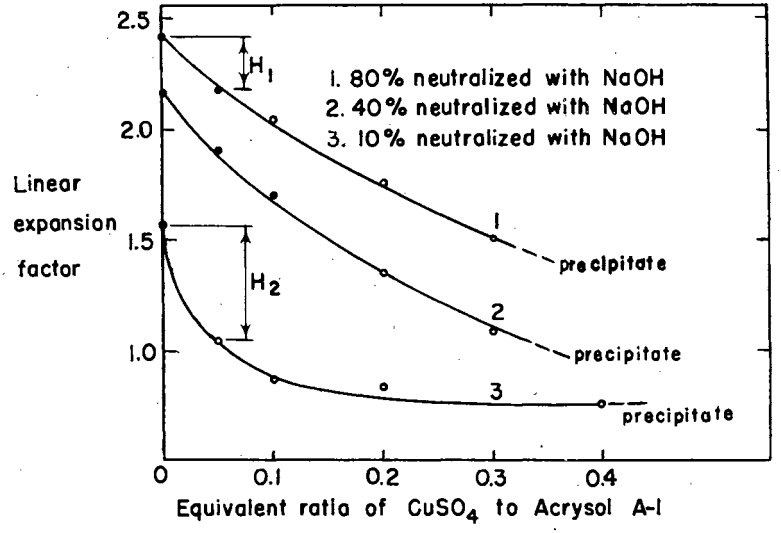

Figure 19. Linear expansion factor of Acrysol A-1 in 0.5% aqueous solution as a function of percent neutralization with sodium hydroxide and of copper sulfate concentration.

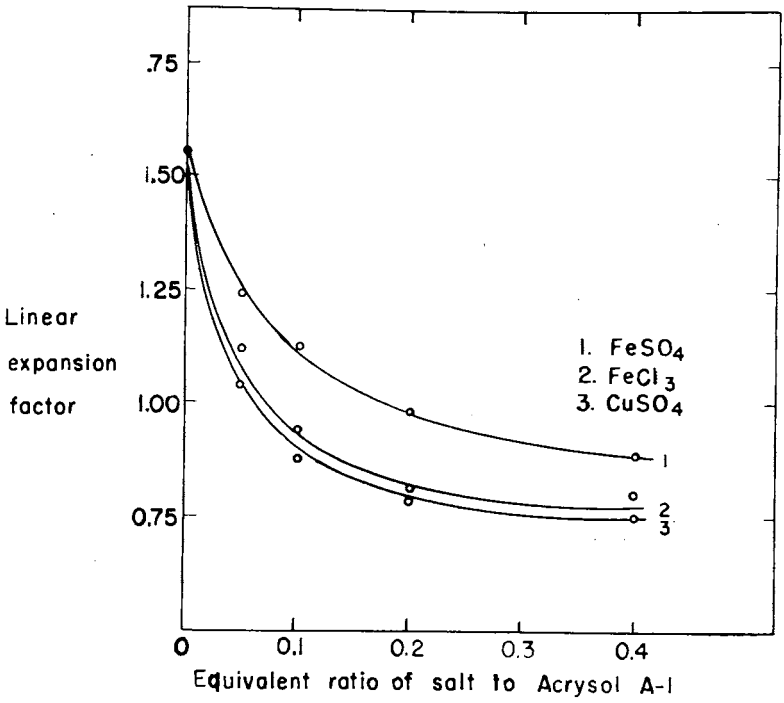

Figure 20. Linear expansion factor of Acrysol A-1 in 0.5% aqueous solution 10% neutralized with sodium hydroxide in the presence of copper and iron salts.

acid molecules at low percentages of neutralization. H_1 is the contraction occurring with a copper-Acrysol A-1 equivalent ratio of 0.05 for 80% neutralization. H_2 is the contraction for the same equivalent ratio of salt to polyacid at 10% neutralization. If the polyacid is first neutralized to enable ionic bonding to the organic cations in the soil and subsequently chelated to stretch the polyacid chains, this relationship between H_1 and H_2 may be significant from the standpoint of economy of the chemicals used to elongate and contract the polyacid chains.

In Figure 20 the concentration caused by copper ions at 10% neutralization is compared with the contractions caused by ferrous and ferric ions. The fact that the ferrous curve now lies above the copper curve, corresponding more closely to the results in Figure 17 than to those in Figure 16, seems to again indicate a greater pH dependency of ferrous chelate formation.

As mentioned previously, the fact that ferric ions precipitated Acrysol A-1 under the conditions represented in Figure 17 is suggestive of inner complex salt formation. To learn more about the water-proofing nature of copper, ferrous and ferric ions with poly-

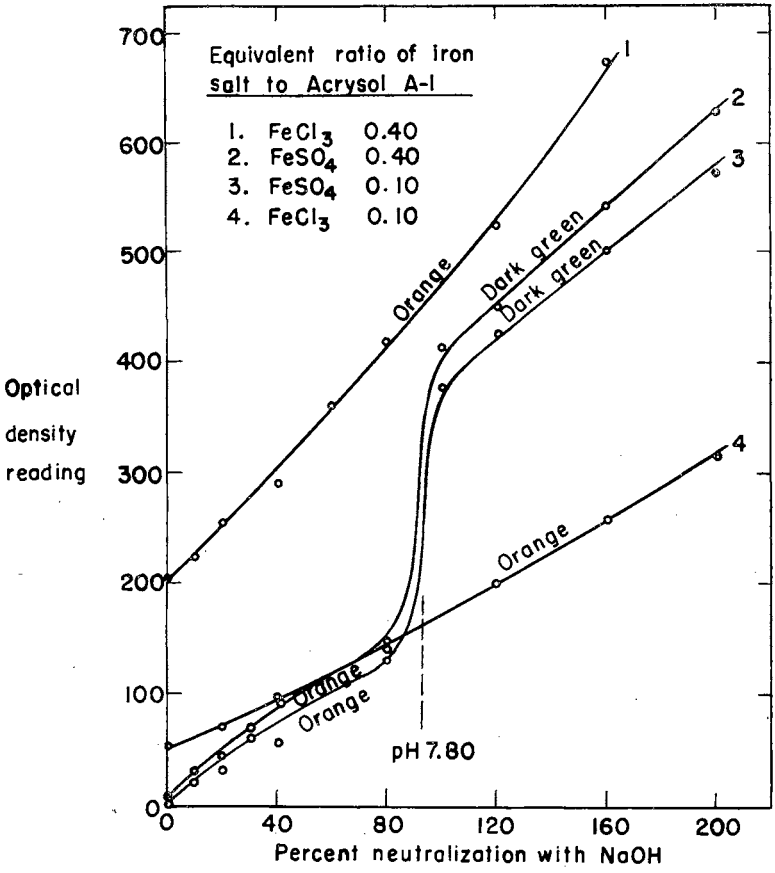

Figure 21. Optical densities of Acrysol A-1 in 0.25% aqueous solution equilibrated with various concentrations of $FeSO_4$ and $FeCl_3$ as a function of neutralization with NaOH.

acrylic acid optical density measurements were made. The use of optical density measurements, now a common identification test for inner complex salts, is based on the work of McKenzie and coworkers (32) and others who found that ionic chelates have adsorption spectra similar to those of the two reactants whereas covalently bonded chelates have adsorption bands characteristic of the chelate and hence of the metal bond.

Figures 21 and 22 show curves obtained by plotting optical density against the percent neutralization of Acrysol A-1 with sodium hydroxide in the presence of various amounts of ferrous, ferric and copper ions. The optical densities shown are the differences between readings of the chelates and of the metal salts. Readings were taken with a Klett Immersion model 800-3 photoelectric colorimeter containing a blue filter.

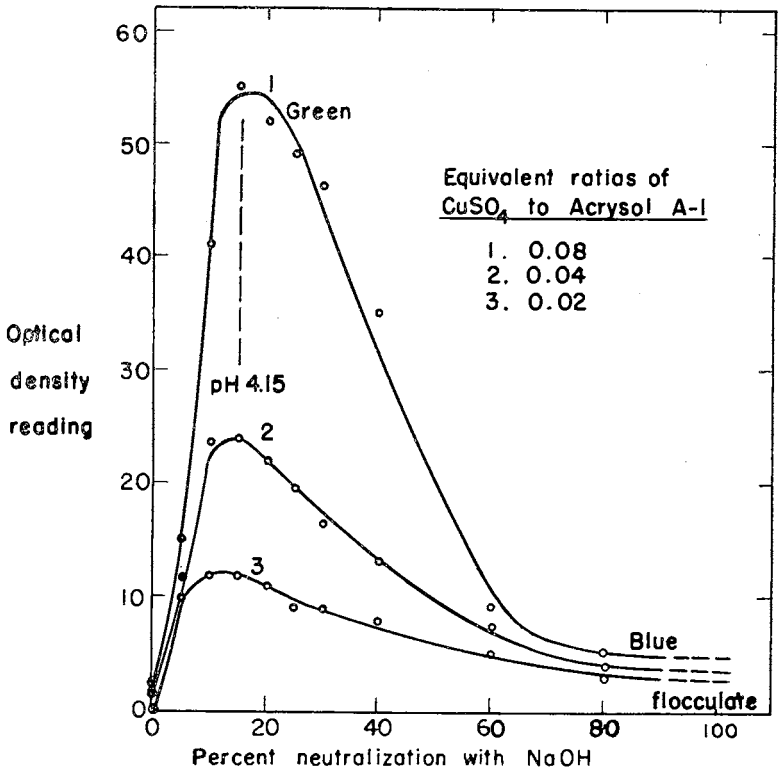

Figure 22. Optical densities of Acrysol A-1 in 2.5% aqueous solution equilibrated with various concentrations of $CuSO_4$ as a function of percent neutralization with NaOH.

It is interesting to compare the optical density curves of Acrysol A-1 in the presence of ferrous and ferric ions, Figure 21. The sudden color change in the presence of ferrous ions at approximately 100% neutralization with sodium hydroxide is apparently caused by an alternate resonance form in the ferrous chelate.

The optical density of the copper chelate (Figure 22) passes through a maximum at about 15% neutralization of Acrysol A-1 with sodium hydroxide. At higher percentages of neutralization the green color of the chelate is gradually replaced by the blue color of copper hydroxide. These curves illustrate the critical dependence of copper chelate formation upon pH, an important factor to consider in its use for soil stabilization. The low concentration of the chelate at low percentages of neutralization is apparently due to the competition of hydrogen ions with copper ions for the polyacrylic acid, whereas at pH values above the optimum for chelation the equilibrium is shifted from the copper chelate to copper hydroxide.

In general, the number of chelate donor groups which can combine with a metal ion corresponds with the coordination number of that

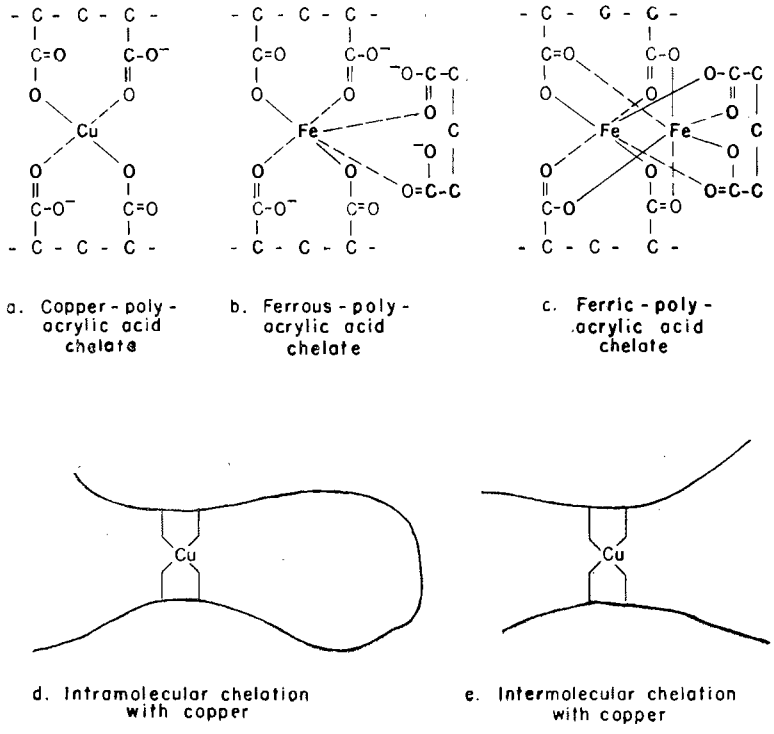

a. Copper - poly - acrylic acid chelate

b. Ferrous - poly - acrylic acid chelate

c. Ferric - poly - acrylic acid chelate

d. Intramolecular chelation with copper

e. Intermolecular chelation with copper

Figure 23. Suggested chelate structures for polyacrylic acid with copper, ferrous and ferric ions.

ion. Copper, with a coordination number of four, is almost always found in a square planar configuration whereas iron, with a coordination number of six, assumes octahedral coordination (24, p. 246). Suggested structures for the copper, ferrous and ferric chelates are shown in Figure 23. In the ferrous chelate (Figure 23b) a color change may be caused by displacement of the C=O double bond when a proton is removed from the carboxylate group by sodium hydroxide. In the structure suggested for the ferric chelate (Figure 23c) there are no carboxylate groups from which protons can be removed and therefore no color change would be possible. The fact that the ferric chelate precipitates more readily than the ferrous chelate (Figure 17) also seems to suggest a structure less polar than that of the ferrous chelate, in accordance with Figures 23b and 23c. Steric limitations to the structure in Figure 23c however have not been investigated.

Whether chelation with copper, ferrous and ferric ions is intramolecular, as represented for the copper ion in Figure 23d, or intermolecular, as in Figure 23e, is probably statistical, depending upon the concentration of the polyacid chains. If the polyacid were used

in sufficient concentration in the soil to permit gelation, i.e. formation of a continuous network structure by intermolecular chelation, the bonding of soil particles would be effected by a continuous macromolecule, providing greater rigidity.

Summary

The mechanisms of soil stabilization with large organic cations and with high polymers have been discussed and an equation has been derived for the shear strength as a function of properties of the polymer.

From the experimental work completed to date it may be concluded that:

1. The immersed strength and air-dry strength of a silty loam treated with a large organic cationic material can be increased by the addition of polyacrylic acid.

2. The effectiveness of the polyacrylic acid is dependent upon its molecular weight. Three samples having average intrinsic molecular weights ranging from 75,000 to 250,000 give increasing strengths with decreasing molecular weight.

3. The hydroxide form of the large organic cation used with polyacrylic acid gives greater strength of the treated soil than does the chloride form.

4. The strength of the cation-polyacid treated soil can be further increased by partial ionization of the polyacid with potassium hydroxide.

5. Cupric, ferrous and ferric ions form inner complex salts with polyacrylic acid, the ferric ion being the most active of the three. Several ferric complexes and slowly soluble ferric salts are presently being evalulated for their ability to increase the strength of the treated soil by reacting with the polyacid slowly enough to permit compaction of the soil and ionic bonding between organic cations and polyacid before tensioning and water-proofing of the polyacid chains by chelation.

Acknowledgment

The subject matter of this report was obtained as part of the research being done under Project 283-S of the Engineering Experiment Station of Iowa State College. This project entitled, "The Loess and Glacial Till Materials of Iowa; an Investigation of Their Physical and Chemical Properties and Techniques for Processing Them to Increase Their All-Weather Stability for Road Construction," is being carried on under contract with the Iowa Highway Research Board and is supported by funds supplied by the Iowa State Highway Commission and the U. S. Bureau of Public Roads.

Literature Cited

1. Davidson, D. T. Exploratory evaluation of some organic cations as soil stabilizing agents. Proceedings, Highway Research Board. Vol. 29, pp. 531-536. 1949.
2. Hoover, James M., and Davidson, D. T. Organic cationic chemicals as stabilizing agents for Iowa loess. Highway Research Board Bulletin 129, pp. 10-25. 1956.
3. Kardoush, F. B., Hoover, J. M., and Davidson, D. T. Stabilization of loess with a promising quaternary ammonium chloride. Paper presented at the 36th Annual Meeting of the Highway Research Board, Washington, D. C., January 7-11, 1957.
4. Hendricks, S. B. Base exchange of the clay mineral montmorillonite for organic cations and its dependence on adsorption due to van der Waals forces. Journal of Physical Chemistry. Vol. 45, pp. 65-81. 1944.
5. Jordan, J. W. Organophilic bentonites, I, Swelling in organic liquids. Journal of Physical and Colloid Chemistry. Vol. 53, pp. 294-306. 1949.
6. Jordan, J. W. Alteration of the properties of bentonite by reaction with amines. Mineralogy Magazine. Vol. 28, pp. 598-605. 1949.
7. Haines, W. B. Studies in the physical properties of soils. II. A note on the cohesion developed by capillary forces in an ideal soil. Journal of Agricultural Science. Vol. 15, pp. 529-535. 1925.
8. Nicholls, R. L. Preliminary investigations for the chemical stabilization of loess in southwestern Iowa. Unpublished M.S. thesis. Iowa State College. 1952.
9. Smallwood, H. M. Limiting law of the reinforcement of rubber. Journal of Applied Physics. Vol. 15, pp. 758-766. 1944.
10. Guth, Eugene. Theory of filler reinforcement. Journal of Applied Physics. Vol. 16, pp. 20-25. 1945.
11. Stearns, R. S., and Johnson B. L. Interaction between carbon black and polymer in cured elastomers. Industrial and Engineering Chemistry. Vol. 43, pp. 146-154. 1951.
12. Szwark, M. The action of carbon black in stabilizing polymeric materials. Journal of Polymer Science. Vol. 19, pp. 589-590. 1956.
13. Einstein, A. Ann. d. Physik. Vol. 19, p. 289. 1906.
14. Einstein, A. Ann. d. Physik. Vol. 34, p. 591. 1911.
15. Guth, E., and Gold O. On the hydrodynamical theory of the viscosity of suspensions. Physical Review. Vol. 53, p. 322. 1938.
16. Robinson, Howard A. High-Polymer Physics. A Symposium. pp. 316-359. Chemical Publishing Company. New York. 1948.
17. Flory, P. J., Rabjohn N., and Shaffer, M. C. Dependence of tensile strength of vulcanized rubber on degree of cross-linking. Journal of Polymer Science. Vol. 4, pp. 435-455. 1949.
18. Flory, P. J. Principles of Polymer Chemistry. Cornell University Press. 1953.
19. Kuhn, W., Hargitay, B., Katchalsky, A., and Eisenberg, H. Reversible dilation and contraction by changing the state of ionization of high polymer acid networks. Nature. Vol. 165, pp. 514-516. 1950.
20. Katchalsky, A., Kunzle, O., and Kuhn, W. Behavior of polyvalent polymeric ions in solution. Journal of Polymer Science. Vol. 5, pp. 283-300. 1950.
21. Katchalsky, A. Problems in the physical chemistry of polyelectrolytes. Journal of Polymer Science. Vol. 12, pp. 159-184. 1954.
22. Katchalsky, A., and Swick, M. Mechanochemistry of ion exchange. Journal of Polymer Science. Vol. 16, pp. 221-234. 1955.
23. Huizenga, Philip, Grieger, F., and Wall, F. T. Electrolytic properties of aqueous solutions of polyacrylic acid and sodium hydroxide. I. Transference experiments using radioactive sodium. Journal of American Chemical Society. Vol. 72, pp. 2636-2642. 1950.

24. Martell, Arthur E., and Calvin, Melvin. Chemistry of the metal chelate compounds. Prentice-Hall, Inc. New York. 1952.
25. Boyd, G. E. Ion exchange. Annual Review of Physical Chemistry. Vol. 2, pp. 309-342. 1951.
26. Mellor, D. P., and Maley, L. Order of stability of metal complexes. Nature. Vol. 161, pp. 436-437. 1948.
27. Iler, R. K. Linear Polymetaphosphates-quaternary ammonium salts. Journal of Physical Chemistry. Vol. 56, pp. 1086-1089. 1952.
28. Kressman, T. R. E., and Kitchener, J. A. Cation exchange with a synthetic phenol and sulphonate resin. Part III. Equilibria with large organic cations. Journal of the Chemical Society, London, pp. 1208-1210. 1949.
29. Terayama, Hiroshi. Viscometric and light scattering behovior of polyelectrolyte solutions in the presence of added electrolytes. Journal of Polymer Science. Vol. 19, pp. 181-198. 1956.
30. Grim, Ralph E. Clay Mineralogy. McGraw-Hill. New York. 1953.
31. Flory, Paul J., and Osterheld, Jean E. Intrinsic viscosities of Polyelectrolytes. Poly-(acrylic acid). Journal of Physical Chemistry. Vol. 58, pp. 653-661. 1954.
32. McKenzie, H. A., Mellor, D. P., Mills, J. E., and Short, L. N. The light adsorption and magnetic properties of nickel complexes. Journal and Proceedings of the Royal Society of New South Wales. Vol. LXXVIII, pt. 3, pp. 70-80. 1944.

Appendix

Properties of Chemicals Used

Commercial Name	Chemical Description	Form	Percent Active Fraction	Equivalent Molecular Weight	Average Intrinsic Molecular Weight	Supplier
Arquad 2HT	Di-hydrogenated tallow dimethylammonium chloride	Isopropanol solution	75	585-605	75,000	Armour Chemical Division
Acrysol A-1	Polyacrylic acid	Aqueous solution	25	72	150,000	Rohm and Haas Company
Acrysol A-3	Polyacrylic acid	Aqueous solution	25	72	250,000	Rohm and Haas Company
Acrysol A-5	Polyacrylic acid	Aqueous solution	25	72		Rohm and Haas Company
Acrysol GS	Sodium salt of Polyacrylic acid	Aqueous solution	12½	94		Rohm and Haas Company
Acrysol G-110	Ammonium salt of polyacrylic acid	Aqueous solution	22	89		Rohm and Haas Company
Acrysol ASE-75	A linear copolymer of acrylic ester with a carboxylic acid	Aqueous solution	40			Rohm and Haas Company
Acrysol ASE-60	A very slightly crosslinked copolymer of acrylic acid	Aqueous emulsion	28			Rohm and Haas Company
Rhoplex AC-33	An acrylic resin	Aqueous emulsion	46			Rohm and Haas Company
Krilium Loamaker	A hydroyzed polyacrylonitrile	Powder				Monsanto Chemical Company

Properties of the Silty Loam*

Chemical Properties:	
Organic matter	0.17%
Carbonates	10.17%
Iron	1.69%
Sulfate content	0.0%
Cation exchange capacity	8.7 me/100 gm.
pH	8.7
Mineralogical Composition of the Clay Fraction: Primarily montmorillonite with smaller quantities of illite and kaolinite.	
Textural Composition:	
Sand	0.4%
Silt	79.8%
Clay	19.8%
Colloidal clay	14.5%
USBPR classification	silty loam

*Laboratory sample 20-2.

IOWA ENGINEERING EXPERIMENT STATION
IOWA STATE COLLEGE
AMES, IOWA